Numerical Simulation of Ship Seakeeping by the SWENSE Approach

B. Alessandrini, P. Ferrant, L. Gentaz

Ecole Centrale Nantes, France

Christian Behrault

Principia, France

ABSTRACT

This paper documents the SWENSE (Spectral Wave Explicit Navier-Stokes Equations) approach, an original method for studying the simulation of 6 DOF ships in nonlinear waves under viscous flow theory. This work has been motivated by the accuracy and efficiency requirements for simulating hulls maneuvering in waves. The validation of the method for a diffraction case is presented and followed by a 2 DOF simulation of a Wigley hull in head regular waves. Results show an overall good agreement with experiments. The accuracy and effectiveness confirm the viability of the method.

KEYWORDS

Navier-Stokes equations, free surface viscous flow, ship in waves, nonlinear diffraction, potential incident flow, SWENS Equations

INTRODUCTION

Performance and seakeeping predictions are usually carried out in towing tank. However, in ship hydrodynamics, Computational Fluid Dynamics (CFD) is more and more used as a practical design tool. Main advantages of CFD are cost and time reduction and easier access to detailed flow field information.

The complexity of simulating the behavior of a ship in seaways was historically overcome by separating the problem in many simpler analysis : resistance, propulsion, maneuvering and seakeeping. However all of those aspects are strongly coupled, CFD only simulates all of those aspects separately using adapted theories :

- Resistance and propulsion analysis are more and more often addressed using viscous flow solvers based on Reynolds Averaged Navier-Stokes Equations (RANSE), because viscosity or flow separation effects play an important role in the physics of those phenomena.
- Maneuvering and seakeeping problems are mainly solved by potential flow theory which is less time consuming and enables an accurate and efficient account of wave propagation phenomena.

However neglecting viscous effects can lead to poor predictions especially for rolling motion. This is why a natural evolution for CFD is to try to address seakeeping and resistance problems within an unified approach by taking into account incident waves in performance predictions.

The classical method used to simulate the viscous flow around a ship advancing in head waves is to impose an incident wave field at the inlet boundary. It is modeled as velocity perturbations which are added to the uniform stream. Those perturbations are usually derived from the linear potential flow solution for free-surface traveling waves. However such simulations require very large computing

resources because grids must be very refined between the location of the structure and the location of the wave generation systems (for structured or non-structured grids used with finite differences or finite volumes). This is indeed necessary to propagate the wave from the paddle to the structure with no noticeable damping. Moreover successive wave reflections on the body or on the paddle affect the incoming wave train and reduce the useable duration of the numerical simulation ; it is indeed very complicated to damp the diffracted field without modifying the incident waves.

Furthermore, the generation of complex wave systems, will be very problematic with this method, especially for 3D sea states. However, RANSE seakeeping simulations of a ship advancing in head regular waves using this basic approach are realizable and have been done recently (Weymouth *et al*., 2005) showing quite accurate results compared to "state of the art" potential simulations.

To overcome these difficulties an original formulation is used here by modifying the initial problem in order to solve the diffracted flow only. It consists in splitting all unknowns of the problem (velocities, pressure and free-surface elevation) into the sum of an incident term and a diffracted term. The incident terms are described explicitly using a nonlinear potential flow model. Thus only the part of the grid in the vicinity of the structure needs to be refined. Far from the body a stretched grid allows an efficient damping of the diffracted flow. In the method presented here called SWENSE (Spectral Wave Explicit Navier Stokes Equations) potential flow theory is used to compute the incident waves while viscous effects are taken into account by using a RANSE solver to obtain the diffracted field in the full domain.

By using this approach it is possible to simulate efficiently and accurately the same incident waves as in potential approaches : regular wave trains, focused waves, irregular sea states in 2D or 3D … Moreover, the duration time of the simulations becomes practically unlimited because the incident waves and the diffracted field are separated so it is quite simple to damp the diffracted field only at the boundaries of the domain.

Forward speed diffraction simulations have been done on a naval combatant in regular nonlinear head waves (Luquet *et al*., 2004) showing accurate results on the diffracted field and the forces components. Moreover the efficiency and accuracy of the method was showed at the last CFD workshop (Luquet *et al*., 2005) where our calculations were shown to be faster of a factor one hundred comparing to classical formulation (with the same level of accuracy on the force coefficients).

The objective of the present work is to extend the applicability of the present approach to six degrees of freedom simulations (Jacquin *et al*., 2005) showing accurate results on roll damping simulations. These developments will give access to full seakeeping calculations on realistic sea states. The first step presented in this work is the simulation of a Wigle with forward speed in head regular waves with two degrees of freedom (pitch and heave).

THE SWENSE APPROACH

This approach has one's origin in the noticing that both a RANS solver and an inviscid solver are not well suited to study wave / body interactions because the first has difficulties in simulating the propagation of gravity waves and the second cannot take into account viscous effects which play an important role close to the body. Obstacles for RANS solvers are numerous. This is indeed necessary to propagate the wave from the paddle to the structure with no noticeable damping or gravity waves propagation requires a fine grid to avoid inherent numerical damping (almost 60 points per wavelength). So meshes of classical RANSE applications to wave / body interactions are quite dense and as a consequence it increases the CPU time requirements. Moreover fast computations are critical when numerical simulations are used as a design optimization tool.

On the other hand it becomes hard to avoid wave reflections at the outside boundaries since defining an open field condition is very

complicated. So successive wave reflections on the body or the paddle affect the incoming wave train and reduce the useable duration of the numerical simulation.

Furthermore, 2D prescribed regular waves are easy to generate but the generation of complex wave systems will be very problematic with this method especially for oblique waves and 3D sea states.

Nevertheless, viscous flow solvers are recognized tools to achieve simulations on still water and inviscid solvers are applied successfully to complex waves generation and propagation. The idea presented here consists of combining those theories in a coupled manner in order to mix their advantages.

Numerical techniques involving the coupling of potential / RANS solvers have been proposed in the past for ship hydrodynamic problems. These studies produced satisfactory results with a great improvement in computational time. Nevertheless those techniques were quite hard to carry out as they were essentially based on domain decomposition with an interface problem complicated to treat. What is more, this decomposition is not very accurate and stable for huge wave amplitudes. That is why the present method couple the potential / RANS solvers directly by a variable decomposition which avoid previous obstacles.

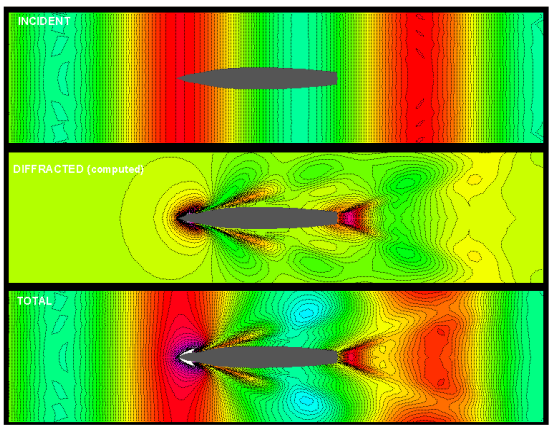

Figure 1: Three steps of the SWENSE approach.

The full simulation of wave / body interactions is decomposed into two successive calculations : a first one consisting of the generation and propagation of waves and a second one for the interaction of those waves with the body. The first problem which contains negligible viscous effects is then solved efficiently and accurately using an method based on potential flow theory. Thus the result obtained is used as the initial field for the RANS computation which gives the complementary part of the flow corresponding to the influence of the structure. As seen on Figure 1, we obtain the total field by summing those two parts.

Using this kind of procedure the propagation of gravity waves is no more calculated in the RANS solver so quite all obstacles are overcome :

The computational time is nearly the same as a computation on still water since the size of the mesh used is equivalent to those of a still water computation. Since the diffracted field is computed alone, it is easy to avoid reflections at the outside boundaries simply by damping it.

The useable incident fields are only limited by the potential model used. So using HOS methods it is possible to generate regular and irregular 3D waves like prescribed focused wave packets or realistic sea-states.

For comparison, at the last CFD Workshop held in Tokyo (2005), the use of our method reduces the CPU time requirement of a factor one hundred on a forward speed diffraction test case even if we assume the fact that using our meshes we do not represent accurately the farfield but only the nearfield and the forces coefficients.

THEORY

In this section, the numerical method is described. Governing equations are presented and followed by boundary conditions. The model used for the incident flow and the numerical method for solving the whole set of equations are presented.

Coordinate system

A space-fixed coordinate system (o-$x_1x_2x_3$), see Figure 2, is defined with the (o-x_1x_2) plane on the still free surface and the z–axis directed

vertically upwards. The origin of the coordinate system is placed at the intersection of the undisturbed free surface and forward perpendicular (FP) of the model and the x_1-axis is directed downstream.

Another coordinate system $(\varepsilon_1, \varepsilon_2, \varepsilon_3)$, fitted to the hull and free surface field is used to define the curvilinear computational domain.

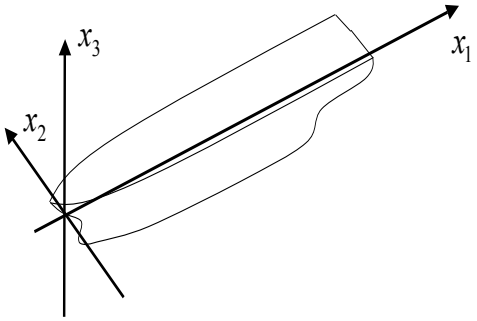

Figure 2: Definition of the coordinate system.

RANS equations

The SWENSE approach is applied here on a viscous flow solver which uses 3D RANS Equations under fully non-linear free-surface boundary conditions.

The RANS equations are first defined in Cartesian coordinates (x_i) and then are written in the non-orthogonal curvilinear coordinates (ε_i) by using a partial transformation. Details of the coordinate transformation can be found in Alessandrini *et al.* (1995).

Thus, the continuity and momentum equations in the transformed space are given by :

$$a_i^k \frac{\partial U^i}{\partial \varepsilon_k} = 0 \tag{1}$$

$$\frac{\partial U^\alpha}{\partial t} + \left(a_i^j \left(U^i - v_g{}^i \right) - \frac{1}{\mathrm{Re}_{eff}} f^j - a_k^i \frac{\partial \upsilon_t}{\partial \varepsilon^i} a_k^j \right) \frac{\partial U^\alpha}{\partial \varepsilon_j} = -a_\alpha^k \frac{\partial P}{\partial \varepsilon_k} + \frac{1}{\mathrm{Re}_{eff}} g^{ij} \frac{\partial^2 U^\alpha}{\partial \varepsilon_j \partial \varepsilon_i} + a_k^i \frac{\partial \upsilon_t}{\partial \varepsilon_i} a_\alpha^j \frac{\partial U^k}{\partial \varepsilon_j} \tag{2}$$

Where :

$P = \hat{P} + \frac{2}{3}\rho k$ is the dynamic turbulent pressure

$\frac{1}{\mathrm{Re}_{eff}} = \frac{1}{\mathrm{Re}} + \upsilon_t$ with ν_t turbulent kinematic viscosity and

$g^{ij} = a_k^i a_k^j$ is the contravariant metric tensor,

$f^j = \frac{1}{J} \frac{\partial}{\partial \varepsilon^i} \left(J g^{ji} \right)$ are the control grid functions,

$v_g{}^i = \frac{\partial x_i}{\partial t}$ are the grid velocities.

SWENS Equations

The previous set of RANS Equations is modified in order to formulate a problem for the nonlinear diffracted flow. Primitive unknowns (Cartesian components of velocity U^i, $i \in \{1,2,3\}$, pressure P and free-surface elevation h) are decomposed as follows :

$$\begin{cases} U^i = U_I^i + U_D^i \\ P = P_I + P_D \\ h = h_I + h_D \end{cases} \tag{3}$$

Variables with the subscripts I and D represent incident and diffracted variables respectively.

This decomposition is then introduced in the set of RANS equations (1) (2) assuming that the incident wave flow fulfils Euler equations:

$$a_i^k \frac{\partial U_D^i}{\partial \varepsilon_k} = 0 \tag{4}$$

$$\begin{aligned} &\frac{\partial U_D^\alpha}{\partial t} + \left(a_i^j \left(U_I^j + U_D^j - v_g{}^i \right) - \frac{1}{\mathrm{Re}_{eff}} f^j - a_k^i \frac{\partial \upsilon_t}{\partial \varepsilon_i} a_k^j \right) \frac{\partial U_D^\alpha}{\partial \varepsilon_j} \\ &- \frac{1}{\mathrm{Re}_{eff}} g^{kk} \frac{\partial^2 U_D^\alpha}{\partial \varepsilon_k{}^2} + a_\alpha^k \frac{\partial P_D}{\partial \varepsilon_k} \\ &= \frac{1}{\mathrm{Re}_{eff}} g^{jk} \left. \frac{\partial^2 U_D^\alpha}{\partial \varepsilon_j \varepsilon_k} \right|_{k \neq l} + a_k^i \frac{\partial \upsilon_t}{\partial \varepsilon_i} a_\alpha^j \frac{\partial}{\partial \varepsilon_j} \left(U_I^k + U_D^k \right) \\ &+ \frac{1}{\mathrm{Re}_{eff}} \left(g^{jk} \frac{\partial^2 U_I^\alpha}{\partial \varepsilon_j \varepsilon_k} + f^j \frac{\partial U_I^\alpha}{\partial \varepsilon_j} \right) - a_j^k \left(U_D^j - a_j^i \frac{\partial \upsilon_t}{\partial \varepsilon^i} \right) \frac{\partial U_I^\alpha}{\partial \varepsilon_k} \end{aligned} \tag{5}$$

We obtain a new set of equations called SWENS Equations where incident variables (dynamic pressure, velocities, free-surface elevations and their gradients) are explicit. Their values are directly computed at each time

step knowing kinematics and interface position of the incident flow. Then, only the diffracted variables are unknowns of the problem and have to be solved by the modified viscous solver.

To conclude, the solution obtained is the solution of a modified problem where incident terms are known and their values are replaced in the SWENS Equations. There are no specific assumptions and the diffracted solution summed with the incident field give the solution of the initial problem.

Modified boundary conditions

The no-slip boundary condition generates the diffracted field from the hull :

$$U_D^i = -U_I^i \tag{6}$$

The modified condition applied on the farfield verifies the decay of the diffracted field far from the body in the same way as previously :

$$U_D^i = 0 \tag{7}$$

Then nonlinear free surface boundary conditions are written in curvilinear coordinates where difftacted unknowns are considered under implicit form :

$$\begin{aligned}&\frac{\partial h_D}{\partial t} + a_1^j\left(\frac{\partial h_D}{\partial \varepsilon_j} + \frac{\partial h_I}{\partial \varepsilon_j}\right)U_D^1 + a_2^j\left(\frac{\partial h_D}{\partial \varepsilon_j} + \frac{\partial h_I}{\partial \varepsilon_j}\right)U_D^2 - U_D^3 \\ &= U_I^3 - \frac{\partial h_I}{\partial t} - a_1^j\left(\frac{\partial h_D}{\partial \varepsilon_j} + \frac{\partial h_I}{\partial \varepsilon_j}\right)\left(U_I^1 - v_g{}^1\right) \\ &-a_2^j\left(\frac{\partial h_D}{\partial \varepsilon_j} + \frac{\partial h_I}{\partial \varepsilon_j}\right)\left(U_I^2 - v_g{}^2\right)\end{aligned} \tag{8}$$

The components of the two vectors tangential and the one normal to the free surface can be respectively expressed using the covariant $a_i = \left(a_{ij}\right)$ and contra-variant $a^i = \left(a_j^i\right)$ vectors as following :

$$t_{ij} = \frac{a_{ij}}{|a_i|}, \begin{vmatrix} i \in \{1,2\} \\ j \in \{1,2,3\} \end{vmatrix}, n_j = \frac{a_j^3}{|a^3|}, \quad j \in \{1,2,3\} \tag{9}$$

Then, the normal and tangential dynamic conditions respectively become :

$$\begin{aligned}&P_D - \rho g h_D \\ &= \rho g h_I - P_I - 2\rho\left(\upsilon + \upsilon_t\right)\frac{a_i^3 a_j^3 a_j^k}{\left|a^3\right|^2}\frac{\partial\left(U_I^i + U_D^i\right)}{\partial \varepsilon_j}\end{aligned} \tag{10}$$

$$\begin{cases}\left(a_j^k a_j^3 a_{1i} + a_j^k a_i^3 a_{1j}\right)\dfrac{\partial U_D^i}{\partial \varepsilon^k} = -\left(a_j^k a_j^3 a_{1i} + a_j^k a_i^3 a_{1j}\right)\dfrac{\partial U_I^i}{\partial x^j} \\ \left(n_j t_{2i} + n_i t_{2j}\right)\dfrac{\partial U_D^i}{\partial x^j} = -\left(n_j t_{2i} + n_i t_{2j}\right)\dfrac{\partial U_I^i}{\partial x^j}\end{cases} \tag{11}$$

Turbulence model

Finally, to close the equations set we used a classical $k-\omega$ turbulence model proposed by Wilcox (1988), introducing a specific dissipation rate ϖ without low Reynolds formulation requirement.

INCIDENT waves

In order to apply the SWENSE method it is necessary to be able to know at each time step all the characteristics of the incident field (velocities, pressure, free surface elevations). A nonlinear model for incident regular wavetrains has been implemented in the present version of the code. Even if the field is only represented in the water, the solution is nevertheless independent of the Navier-Stokes grid and can be computed everywhere. Some attributes were essential in the choice of this model. Especially, in the SWENSE method, values of the incident field will be possibly needed above the undisturbed incident free surface, as the total free surface elevation can indeed be higher than the incident elevation. Both wave model described below gives access to a regular continuation of the incident fluid flow above the incident free surface, allowing an effective implementation of the SWENSE scheme. Furthermore, the velocity field generated by this method is infinitely derivable on the whole space and this continuity is essential for the implementation of the equations and the behavior of the

computations.

So we consider a 2D non-linear regular incident wave train. To compute it, an algorithm based on the stream function theory (Rienecker & Fenton, 1981) has been implemented. This algorithm has been chosen as it can generate the solution of steadily progressing periodic waves on irrotational flow over a horizontal bed for a wide range of depth (but not for the solitary wave limit), amplitudes and wavelengths (in the limit of breaking waves) with huge accuracy (computer accuracy in fact) and fast computations. Figure 3 shows the successive wave profiles of a regular wave at increasing steepnes. For the last profiles on which the crest is very angular, 64 modes were needed to reach the computer accuracy although only 15 are required for most common steepnesses.

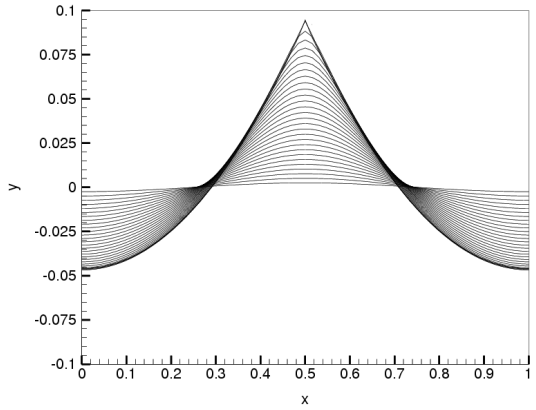

Figure 3: Regular wave profiles up to the Stokes limit.

This precision can be reached since the numerical method has as its only approximation the truncation of the Fourier series. Moreover, the computational time needed to obtain the solution of the incident field at each time step is negligible comparing to a classical RANSE iteration (less than 0.002 %).

It has been developed using potential theory and gives the numerical solution of steadily progressing periodic waves on irrotational flow over a horizontal bed. No analytical approximations are made. This method is based on the decomposition of the current function using Fourier series. The application of the nonlinear free surface boundary conditions and the Laplace equation gives a set of nonlinear equations from which unknowns are the amplitudes of each mode of the Current Fourier series and the free surface elevation at each collocation point. Since the number of collocation points is the same as the number of modes in the Fourier series, an iterative scheme based on a Newton method is then used to solve the nonlinear set of equations. The initial state is the linear solution based on a Airy wave and then successive results are obtained to converge to the fully nonlinear solution.

Thus, with x_1 the horizontal coordinate and x_2 the vertical coordinate, the origin of the coordinate system is placed on the sea bed and moves at the same velocity than the waves. Considering this coordinate system, the movements of the progressing wave are steady. The velocity potential is then given by :

$$\begin{cases} \phi(x_1,x_2,t) = \sum_{i=0}^{n} \phi_i(x_1,x_2,t) \\ \phi_i(x_1,x_2,t) = B_i \dfrac{\cosh(ikx_2)}{\cosh(ikD)} \cdot \sin\left(ik\left(x_1 - ct\right)\right) \end{cases} \quad (12)$$

And the free surface elevation by :

$$\eta(x_1,x_2,t) = \frac{A_0}{2} + \sum_{i=1}^{n} A_i \cos\left(ik\left(x_1 - ct\right)\right) \quad (13)$$

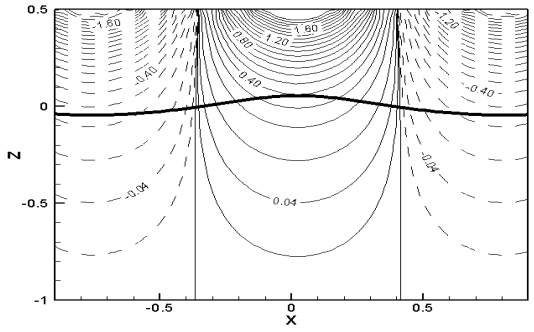

Figure 4: Contouts of the axial velocity in the whole space for $2A = 0.1$, $\lambda = 1.5$. The bold line represents the free surface.

Even if the field is only represented in the water, the solution is nevertheless independent

of the Navier-Stokes grid and can be computed everywhere. This attribute is essential because in the SWENSE method, values of the incident field will be possibly needed above the undisturbed incident free surface. That is why this point is decisive for the choice of the incident field model. Figure 4 shows the axial velocity field to demonstrate the continuity of the wave field under, through and also upon the undisturbed free surface.

Six Degrees of Freedom Ship Motion

The solver must be able to compute the motions of the ship under forces computed at each time step. This is done by solving the standard Euler's law in the body fixed coordinate frame centered on *G*. The six components of ship velocity and position are then obtained and allow to move the ship by moving the grid, whereas the velocities are used for boundary conditions on the hull.

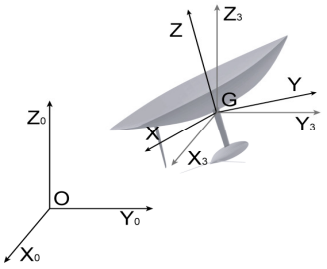

Figure 5: Fixed reference and body fixed axis

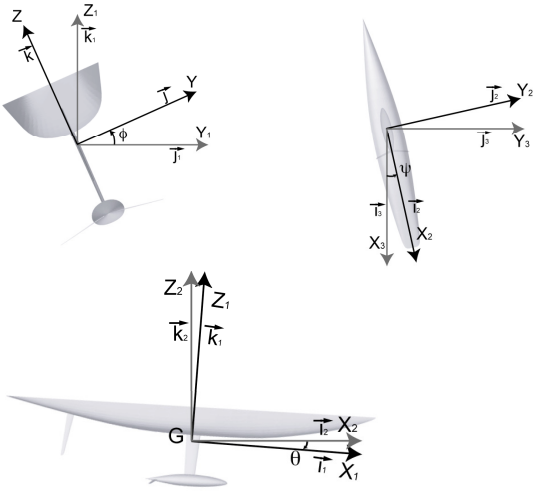

Figure 6: Decomposition of the rotation of the ship.

Navier-Stokes equations are solved is the fixed general axis center on 0 *(R_0)*. This coordinate frame is Galilean, so acceleration terms of the fluid in the Navier-Stokes equations do not have to be taken into account, and then reduce the complexity of the problem.

The Euler's laws are solved in the body fixed coordinate frame center on G *(R_G)*.

The rotation matrix used to transform coordinates from the fixed coordinate frame to the body fixed coordinate frame is defined by:

$$P_{R_3 \to R} = P_{R_1 \to R}\, P_{R_2 \to R_1} P_{R_3 \to R_2} \tag{14}$$

The ship motion equations are written using the Euler's law :

$$m\left(\frac{d\vec{V}_{G/R}}{dt} + \vec{\omega}_R \wedge \vec{V}_{G/R}\right) = \vec{F}_{/R} \tag{15}$$

$$I_R \frac{d(\vec{\omega}_R)}{dt} + \vec{\omega}_R \wedge (I_R \vec{\omega}_R) = \vec{M}_{G/R}$$

Where

m is the mass of the ship

I_R is the inertial matrix of the ship

$\vec{V}_{G/R}$ is the velocity vector of the center of gravity

$\vec{\omega}_R$ is the angular velocity vector

$\vec{F}_{/R}$ is the total forces acting the ship (hydrodynamic, aerodynamic, gravitational and external forces)

$\vec{M}_{G/R}$ is the total momentum acting on the ship

After calculation of velocity components $\vec{V}$, positions of the ship are then directly integrated from ship velocities.

The integration scheme is a predictor corrector scheme, based on explicit and implicit second order multi-step methods (Adams Baschford and Adams Moulton methods).

First results on maneuverability simulations have been presented by Jacquin *et al.* (2006)

showing encouraging results.

NUMERICAL DETAILS

The SWENSE method is applied to the ICARE solver (Alessandrini and Delhommeau, 1995) developed through the support of the French Navy. It solves the Reynolds Averaged Navier-Stokes Equations written in convective form in an unsteady curvilinear computational space fitted at each iteration to the hull and to the free surface. Fully non linear free surface boundary conditions are implemented using an efficient fully coupled algorithm. Turbulence effects are taken into account through classical k-ω turbulence model. An original fully-coupled method is used to solve the discretised set of equations : at each iteration all equations (RANS Equations, pressure equation, free-surface boundary conditions, no-slip conditions) are assembled in a single large and sparse linear system which is solved using a bi-CGSTAB algorithm with an incomplete LU preconditioning. This method offers a better accuracy and efficiency than weak coupled algorithms (SIMPLER, PISO), especially for the convergence of the velocity-pression coupling.

Finally the combination of incident potential flow and RANS solvers for the diffracted problem can be summarized as follows : At each time step of the computation the geometry of the fluid domain is updated. The kinematics of the incident wave flow is calculated on this updated grid and then the diffracted problem defined by the set of SWENS Equations (4) to (11) is solved using the viscous flow software described previously. The diffracted solution is then summed with the incident terms in order to obtain the total field. Considering the total free surface elevation it is now possible to update the fluid domain again.

RESULTS

Regular Head Waves on the DTMB 5415

The numerical procedure has been further developed to simulate the forward speed diffraction on a naval combatant in regular nonlinear head waves (Luquet *et al*., 2004) showing accurate results on the diffracted field and the forces components. Unsteady resistance, heave force, pitch moment, nominal wake and free-surface elevations have been compared to experiments by Gui *et al*. (2001) and the efficiency and accuracy of the method was showed at the last CFD workshop (Luquet *et al*., 2005) where our calculations were shown to be faster by a factor one hundred comparing to classical formulation (with the same degree of accuracy on the force coefficients). Results on the DTMB5415 presented here concern the added resistance in waves compared to experiments. This results are quite difficult to obtain and show the accuracy of our formulation.

We will focus on the resistant coefficient (C_T) , heave force coefficient (C_H) , pitch moment coefficient (C_M) defined as follows :

$$C_T(t)=\frac{F_X(t)}{0.5\rho U^2 S} \quad C_H(t)=\frac{F_Z(t)}{0.5\rho U^2 S} \quad C_M(t)=\frac{M_Y(t)}{0.5\rho U^2 SL} \qquad (16)$$

where F_X , F_Y , M_Y and z are the measured time-varying resistance, heave force, pitch moment and free-surface elevation, respectively. S is the wetted surface area for the static condition and ρ is the water density. The previous variables are compared to experiments in terms of Fourier components.

Results on DTMB5415

In the present computation the medium amplitude test case of the experiments ($\lambda/L=1.5$, $Ak=0.025$ and $Fn=0.28$) has been simulated using the regular wave model in order to evaluate the added resistance in head waves. Added resistance due to waves refers to ocean waves and is not to be confused with wave making resistance. Ocean waves cause the ship to expend energy by various effects : for example the wetted surface area of the hull increases so causes added viscous resistance. This component of resistance can be very significant in high sea states and has a particular nonlinear behavior.

Classically, the added resistance in heading waves is obtained by subtracting the still water resistance from the measured mean total resistance at the speed concerned. So, two computations have been done with the same conditions for trim and heave at the same Froude number for each steepness at three wavelength. Table 1 resumes the results obtained. The error is computed as $(num - \exp)/\exp * 100$ and the last column represents the amplitude of the added resistance comparing to the total mean resistance.

Table 1: Added resistance compared to experiments.

			$C_{T,add}$			
Fn	*Ak*	λ/Lpp	Num.	Exp.	Err.(%)	$C_{T,add}/C_{T,0}$ (%)
0.28	0.025	0.5	0.00002	0.000013	35	0.2
		1.0	0.00022	0.00015	46	2.6
		1.5	0.00042	0.00040	5	4.5
	0.05	0.5	0.00022	0.00017	29	2.5
		1.0	0.00085	0.0008	6	8.8
		1.5	0.00179	0.00178	1	17
	0.075	0.5	0.00043	0.00041	5	4.5
		1.0	0.00182	0.00192	5	17
		1.5	0.00392	0.00401	2	31

As expected it appears that the added resistance in heading waves is positive and increases following the waves amplitude from 0.2 % to 31 % of the mean total resistance. It varies as the squared wave amplitude for all of the cases presented in this table (if the numerical accuracy is sufficient).

First computations have been done using the classical steepness $Ak = 0.025$ and the results were quite inaccurate. But considering the amplitude of the added resistance compared to the total mean resistance, we have noticed that it was only 2-5 % of $C_{T,0}$. Moreover, the uncertainty of the numerical code appears in the twice computations used to deliver the added resistance, so is multiplied by a factor two about the added resistance. Finally it is obvious that trying to obtain accurate prediction of the added resistance at this steepness is inappropriate as the result is under the uncertainty of the numerical code.

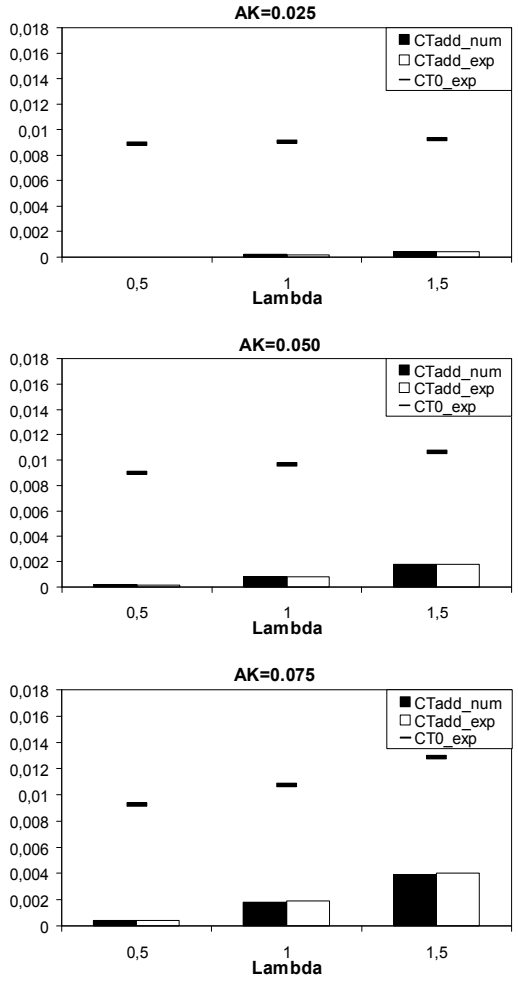

Figure 7: Illustration of Table 1.

Computations at higher steepness (0.05 and 0.075) show accurate predictions of the added resistance (error below 5 %) as the ratio $C_{T,add}/C_{T,0}$ is up to 10 %.

Table 2 presents the results for increasing Fn at $Ak = 0.025$ and $\lambda / L_{pp} = 1.5$. The behavior of the added resistance is well predicted by our method with a small discrepancy at low Froude number. The added resistance decreases regularly with increasing Froude number.

Wigley with 2 DOF in regular head waves

The method is applied here to the interaction of a nonlinear regular wave train with a ship with two degrees of freedom (pitch and heave) in deep water. The selected geometry is a Wigley hull and is supposed to have a forward motion at constant speed.

Table 2: Added resistance compared to experiments for

		$C_{T,add}$	
		Num	Exp
Fn	0.19	0.00073	0.00091
	0.28	0.00042	0.00040
	0.34	0.00038	0.00040
	0.41	0.00031	0.00029

$Ak = 0.025$ and $\lambda / L_{pp} = 1.5$.

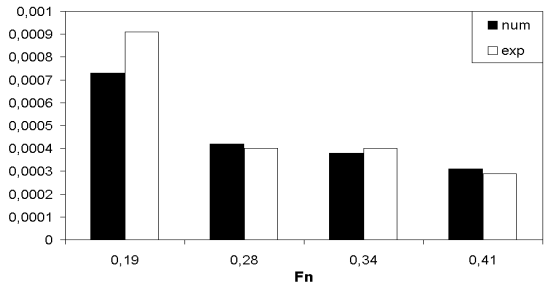

Figure 8: Illustration of Table 2

This geometry has been chosen because many experiments have been carried out in the Delft University of Technology report by Journee (1992). The validation data includes forward speed diffraction, forced heave or pitch and the three degrees of freedom at forward speed. All measurements have been done for four wigley hulls and many incoming wave amplitudes and wavelengths. The incident field is always a regular wave train.

First computations have been carried out for the forward speed diffraction case and results on the first harmonic forces are shown on Table 3. Simulations have been done for a non-dimensional incoming wave amplitude $H/L_{pp} = 0.01734$ at a Froude number $Fn = 0.3$. As expected results are excellent so we are confident on the ability of our method to predict the behaviour of the hull with degrees of freedom.

Simulations including the two degrees of freedom have then been carried out. Pitch θ and heave β motions are expressed respectively in terms of the coefficients Y3 and Y5 :

$$Y_3(t) = \frac{\beta(t)}{2A} \qquad Y_5(t) = \frac{\theta(t)}{2Ak} \qquad (44)$$

Table 3: Amplitude of the first harmonic of the resistance C11 , the heave force C13 and the pitch moment C15.

	λ/L =0.5		λ/L =1		λ/L =2	
	num	exp	num	exp	num	exp
C_{11}	0.0625	0.066	0.247	0.259	0.710	0.713
C_{13}	0.108	0.118	0.210	0.205	0.593	0.577
C_{15}	0.0272	0.026	0.304	0.316	0.634	0.658

Figure 9 shows the wave pattern for λ/L = 1, and Figure 10 the associated motions witch reach a periodic state. Notice that 12 periods of incoming waves have been computed in less than 10 hours using a light mesh (covering an half domain) of 120 000 nodes. It is noticeable that the duration of the simulation in waves using the SWENSE method is the same as a classical RANSE simulation. It is indeed quite not much time consuming to realize resistance tests on waves than on still water using this approach. The duration of computations is considerably reduced comparing to classical approach.

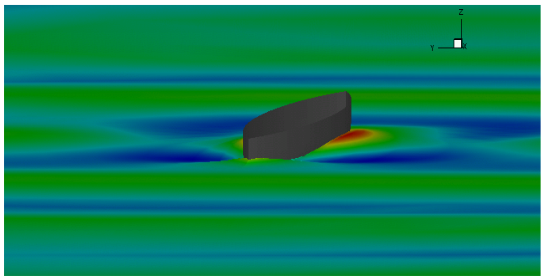

Figure 9: Wave pattern of the Wigley hull in head regular waves free to heave and pitch with forward speed for $\lambda / L_{pp} = 1$

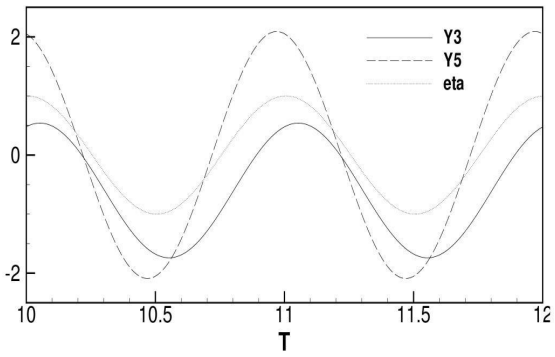

Figure 10: Time history of heave (solid line) and pitch line) for $\lambda / L_{pp} = 1$.

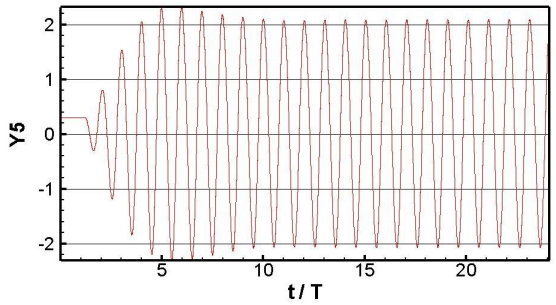

Figure 11: Predicted pitch motion on 24 incoming waves.

Table 4: Amplitude and phase of the heave and pitch coefficients.

	EXP	SWENSE	Strip Theory
Y3	1.28	1.14	1.31
ϕ_{Y3}	343	335	343
Y5	2.21	2.09	1.5
ϕ_{Y5}	13	13	45

Moreover, Figure 11 shows the predicted pitch motion for a long simulation (almost 24 incoming waves) and it is clear that the motion is well established. The signal is fully periodic which illustrates the fact that the absorption of the diffracted field is efficient so accurate long simulations will be possible with no particular care. Table 4 gives values of the amplitude and phase of the first harmonic of the pitch and heave coefficients. Results from experiments, present approach and strip theory computations are given showing the ability of the SWENSE approach to catch the ship motions with accuracy even on this light mesh. It is clear that results from our method improve those coming from strip theory at this resonant case.

CONCLUSION AND FUTURE WORK

In this paper SWENSE method has been extended to simulations with DOF on regular waves by solving the motions of the ship under forces computed at each time step. First comparison even on a light mesh seems to give accurate results on motion coefficients with low CPU time requirements. In addition, the irregular waves will be added to the model by interfacing an advanced HOS model (Bonnefoy, 2003; Bonnefoy *et al.*, 2004; Ducrozet *et al.*, 2005) with the software solving SWENSE equations. The characteristics of accuracy and efficiency will be studied using this new wave model and detailed comparisons with experiments will be undertaken and presented in the near future.

REFERENCES

Alessandrini, B., Delhommeau, G., "A multigrid velocity-pressure-free surface elevation fully coupled solver for calculation of turbulent incompressible flow around a hull", Proceedings of the 9th International Conference on Numerical Methods in Laminar and Turbulent Flows, Atlanta, 1995, pp. 1173-1184.

Bonnefoy, F., "Modélisation expérimentale et numérique des états de mer complexes", PhD thesis, Ecole Centrale de Nantes, 2003.

Bonnefoy, F., Le. Touzé, D., and Ferrant, P., "Generation of fully-nonlinear prescribed wave fields using a high-order spectral model", In Proc. 14th International Offshore and Polar Engineering Conference, Toulon, France, May 2004

Ducrozet, G., Le Touzé, D., Bonnefoy, F., Ferrant, P., « Development of a fully non-linear water wave simulator based on higher order spectral theory", Proceedings of the 20th International Workshop on Water Waves and Floating Bodies, Longyearbayen, 2005.

Gui, L., Longo, J., Metcalf, B., Shao, J., Stern, F., "Forces, Moment and Wave Pattern for Naval Combatant in Regular Head Waves", Proceedings of the 23rd Symposium on Naval Hydrodynamics, 2001.

Jacquin, E., Guillerm, P.E., Derbanne, Q., Boudet, L., Alessandrini, B., "Simulation d'essais d'extinction et de roulis forcé à l'aide d'un code de calcul Navier-Stokes à surface libre instationnaire", Proceedings of the 10th journées de l'hydrodynamique, Nantes, 2005.

Jacquin, E., Guillerm, P.E., Drouet, A., Perdon, P., "Simulation of unsteady ship maneuvering using free-surface RANS solver", In Proc. 26th Symposium on Naval Hydrodynamics, Rome, 2006.

Journee, J. M. J.. "Experiments and calculations on four Wigley hullforms", Delft University of Technology, Ship Hydrodynamic Laboratory, Report 909, 1992.

Luquet, R., Gentaz, L., Ferrant, P., Alessandrini, B., "Viscous

flow simulation past a ship in waves using the SWENSE approach", Proceedings of the 25th Symposium on Naval Hydrodynamics, St John, 2004.

Luquet, R., Jacquin, E., Guillerm, P.E., Gentaz, L., Ferrant, P., Alessandrini, B., "RANSE with free surface computations around fixed and free DTMB 5415 model, in still water and in waves", Proceedings of the CFD Workshop, Tokyo, 2005.

Rienecker, M.M.; Fenton, J.D., "A Fourier approximation method for steady water waves", Journal of Fluid Mechanics, Vol. 104, 1981, pp. 119-137.

Weymouth, G.D.; Wilson, R.V., Stern, F., "RANS Computational Fluid Dynamics Predictions of Pitch and Heave Ship Motions in Head Seas", J. Ship Research. Vol. 49, N°2, pp.80-97, 2005.

Wilcox, D., C., "Reassessment of the scale-determining equation for advanced turbulence models", 1988, AIAA journal, Vol. 26, pp. 1299-1310.